The Nucleus **51**, No. 4 (2015) 411-417

www.thenucleuspak.org.pk

The Nucleus

ISSN 0029-5698 (Print)
ISSN 2306-6539 (Online)

Heat and Mass Transfer Over an Unsteady Stretching Permeable Surface with Non-Uniform Heat Source/Sink and Thermal Radiation

Aurangzaib*, S.M. Murshid and S.A. Urooj

Department of Mathematical Sciences, Federal Urdu University of Arts, Science and Technology, Gulshan-e-Iqbal, Karachi, Pakistan

ARTICLE INFO

Article history :
Received : 27 January, 2014
Revised : 9 October, 2014
Accepted : 25 October, 2014

Keywords :
Heat and mass transfer
Heat source/sink
Thermal radiation

ABSTRACT

In this study an analysis has been done to investigate the combined effects of heat and mass transfer over an unsteady stretching permeable surface with non-uniform source/sink and thermal radiation. The transformed nonlinear boundary layer equations are solved numerically by applying Keller-box method. The numerical results are compared and found to be in good agreement with previously published results under special cases. Finally, the influence of various embedded flow parameters on local skin friction, local Nusselt number and local Sherwood number have been analyzed through graphs carefully.

1. Introduction

Combined heat and mass transfer problems are of importance in many processes and have therefore, received a considerable amount of attention in recent years. In processes such as drying, evaporation at the surface of a water body, energy transfer in a wet cooling tower and the flow in a desert cooler, heat and mass transfer occur simultaneously. Possible applications of this type of flow can be found in many industries. For example, in the power industry, among the methods of generating electric power is one in which electrical energy is extracted directly from a moving conducting fluid. Since the pioneering study by Crane [1] who presented an exact analytical solution for the steady two-dimensional stretching of a surface in a fluid, many authors have been considered various aspect of the problem such as heat source, thermal radiation. Therefore, any research focusing on the solution of these problems always excites researchers and deserves a special attention [2-11].

Thermal radiation effects may play an important role in controlling heat transfer in polymer processing industry where the quality of the final product depends on the heat controlling factors to some extent. High temperature plasmas, cooling of nuclear reactors, liquid metal fluids, and power generation systems are some important applications of radiative heat transfer from a vertical wall to conductive gray fluids. If the entire system involving the polymer extrusion process is placed in a thermally controlled environment, then radiation could become important [12]. Pal and Malashetty [13] have presented similarity solutions of the boundary layer equations to analyze the effects of thermal radiation on stagnation point flow over a stretching sheet with internal heat generation or absorption. The effect of radiation on heat transfer problems have been studied by [14-16] They analyzed heat and mass transfer in two-dimensional stagnation-point flow of an incompressible viscous fluid over a steady stretching vertical sheet in the presence of buoyancy force and thermal radiation. Yusof et al. [17] studied unsteady MHD flow over a stretching sheet in the presence of radiation effect.

The heat generation or absorption may be due to chemical reaction and/or dissociation effects in the flowing fluid. The presence of heat generation or absorption may alter the temperature distribution in the fluid which in turn affects the particle deposition rate in systems such as nuclear reactors, electronic chips, and semiconductor wafers. The exact modeling of internal heat generation or absorption is difficult but some simple mathematical models may express its average behavior for most physical situations. Heat generation or absorption has been assumed to be constant, space dependent or temperature dependent. Abo-Eldahab and El-Aziz [18] included the effect of non-uniform heat source /sink on the steady heat transfer with suction/ blowing. Pal and Mondal [19] examined the effect of non-uniform heat source/sink and variable viscosity on MHD non-Darcy mixed convection heat transfer over a stretching sheet embedded in a porous medium in presence of Ohmic dissipation. Recently, Pavithra and Gireesha [20] studied the boundary layer flow over an exponentially stretching heat on dusty fluid with heat generation/ absorption and viscous dissipation.

The above studies deal with a steady flow only.

* Corresponding author : zaib20042002@yahoo.com

However, in some cases the flow field and heat transfer can be unsteady due to sudden stretching of the flat sheet or by a step change of temperature of the sheet. When the surface is impulsively stretched with certain velocity, the inviscid flow is developed instantaneously. However, the flow in the viscous layer near the sheet is developed slowly, and it becomes a fully developed steady flow after a certain instant of time. The flow problem caused by the impulsive stretching of a sheet has been investigated by Na and Pop [21]. They analyzed the unsteady flow past a wall which starts impulsively to stretch from rest using both numerical and series solution method. Wang et al. [22] investigated impulsive stretching of a surface in a viscous fluid. Using perturbation they analyzed the complete transient behavior of the unsteady viscous flow caused by stretching surface. Elbashbeshy et al. [23] studied the heat transfer over an unsteady stretching surface with internal heat generation. Ishak et al. [24] investigated heat transfer over an unsteady stretching permeable surface with prescribed wall temperature. Pal [25] studied heat transfer over an unsteady stretching permeable surface. Recently, Seini [26] investigated the boundary layer flow over an unsteady stretching sheet with non-uniform heat source and chemical reaction.

In this paper, we consider the problem of heat and mass transfer over an unsteady permeable stretching surface with radiation effect and non-uniform heat source/sink. To the best of our knowledge, this problem has yet not been considered.

2. Mathematical Formulation

Consider the unsteady laminar boundary layer flow with heat and mass transfer over a stretching permeable surface in a quiescent viscous and incompressible fluid. At time $t=0$, the sheet is impulsively stretched with the velocity $U_w(x,t)$ along the $x-$axis. The positive x coordinate is measured along the stretching surface in the direction of motion and the positive y coordinate is measured normal to the sheet in the outward direction toward the fluid. Under the above assumptions along with the boundary layer approximations, the equations that describe the physical situation are given by

$$\frac{\partial u}{\partial x}+\frac{\partial v}{\partial y}=0 \tag{1}$$

$$\rho\left(\frac{\partial u}{\partial t}+u\frac{\partial u}{\partial x}+v\frac{\partial u}{\partial y}\right)=\mu\frac{\partial^2 u}{\partial y^2} \tag{2}$$

$$\frac{\partial T}{\partial t}+u\frac{\partial T}{\partial x}+v\frac{\partial T}{\partial y}=\frac{\kappa}{\rho c_p}\frac{\partial^2 T}{\partial y^2}-\frac{1}{\rho c_p}\frac{\partial q_r}{\partial y}+\frac{q'''}{\rho c_p} \tag{3}$$

$$\frac{\partial C}{\partial t}+u\frac{\partial C}{\partial x}+v\frac{\partial C}{\partial y}=D\frac{\partial^2 C}{\partial y^2} \tag{4}$$

where u and v are the $x-$ and $y-$components of the velocity vector, μ is the fluid viscosity, ρ is the fluid density, κ is the fluid thermal conductivity, c_p is the heat capacity at constant pressure, and D is the coefficient of mass diffusivity, respectively. The appropriate boundary conditions for the above boundary layer equations are

$$\begin{aligned}&u=U_w(x,t), v=V_w, T=T_w, C=C_w \quad \text{at} \quad y=0\\&u\to 0, T\to\infty, C\to\infty \quad \text{as} \quad y\to\infty\end{aligned} \tag{5}$$

The non-uniform heat source/sink, q''', is modeled as [25]

$$q'''=\frac{\kappa U_w(x,t)}{x\upsilon}\left[A^*\left(T_w-T_\infty\right)f'+\left(T-T_\infty\right)B^*\right] \tag{6}$$

where A^* and B^* are the coefficient of space and temperature-dependent heat source/sink, respectively.

We assume that the stretching velocity $U_w(x,t)$ the surface temperature $T_w(x,t)$ and the surface concentration $C_w(x,t)$ are of the form:

$$U_w(x,t)=\frac{ax}{1-ct},\ T_w(x,t)=\frac{bx}{1-ct},\ C_w(x,t)=\frac{bx}{1-ct} \tag{7}$$

Where a,b and c are positive constants having dimension time^{-1} with $ct<1$. $V_w=-\left(\upsilon U_w/x\right)^{1/2}f_w$ is suction/injection parameter; $V_w>0$ for suction and $V_w<0$ for injection.

The equation of continuity is satisfied if we choose a stream function $\psi(x,y,t)$ such that

$$u=\frac{\partial\psi}{\partial y},\qquad v=-\frac{\partial\psi}{\partial x}$$

Using the following similarity transformation [24, 25].

$$\eta=\sqrt{\frac{a}{\upsilon(1-ct)}}y,\ \psi=\sqrt{\frac{a\upsilon}{(1-ct)}}xf(\eta),\ T=T_\infty+\frac{bx}{(1-ct)}$$

$$\cdot\theta(\eta),\ C=C_\infty+\frac{bx}{(1-ct)}\phi(\eta) \tag{8}$$

Using the Rosseland approximation (Raptis [27]), the radiation heat flux is given by

$$q_r=-\frac{4\sigma^*}{3k^*}\frac{\partial T^4}{\partial y} \tag{9}$$

where σ^* and k^* are the Stefan-Boltzmann constant and the mean absorption coefficient, respectively. As done by Raptis [27], temperature differences within the flow are assumed to be sufficiently small so that T^4 may be expressed as a linear function of temperature T using a truncated Taylor series about the free stream temperature T_∞ i.e.,

$$T^4 \approx 4T_\infty^3 T - 3T_\infty^4 \tag{10}$$

Using (8), Equations (2)-(4) can be written as

$$f''' + ff'' - f'^2 - A\left(f' + \frac{1}{2}\eta f''\right) = 0\,, \tag{11}$$

$$\frac{(1+R)}{\Pr}\theta'' + f\theta' - f'\theta - A\left(\theta + \frac{1}{2}\eta\theta'\right) \cdot \frac{1}{\Pr}\left(A^* f' + B^*\theta\right) = 0 \tag{12}$$

$$\frac{1}{Sc}\phi'' + f\phi' - f'\phi - A\left(\phi + \frac{1}{2}\eta\phi'\right) = 0\,. \tag{13}$$

where prime denote differentiation with respect to η, $A = c/a$ is an unsteadiness parameter, $Pr = \mu c_p/\kappa$ is the Prandtl number, $R = 16\sigma^* T_\infty^3/3\kappa k^*$ is the radiation parameter, $Sc = \upsilon/D$ is Schmidt number. The boundary conditions (5) becomes

$$\begin{aligned} &f(0) = f_w, \quad f'(0) = 1, \quad \theta(0) = 1, \quad \phi(0) = 1, \\ &f'(\infty) \to 0, \quad \theta(0) \to 0, \quad \phi(0) \to 0. \end{aligned} \tag{14}$$

with $f_w > 0$ and $f_w < 0$ corresponding to suction and injection, respectively.

The quantities of physical interest are the local skin-friction coefficient; local Nusselt number and the local Sherwood number are defined as

$$C_{fx} = \frac{2\tau_w}{\rho U_w^2}, \qquad Nu_x = \frac{xq_w}{\kappa(T_w - T_\infty)}, \qquad Sh_x = \frac{xm_w}{\rho D(C_w - C_\infty)} \tag{15}$$

where the wall shear stress τ_w, surface heat flux and mass concentration are given by

$$\tau_w = \mu\left(\frac{\partial u}{\partial y}\right)_{y=0}, \quad q_w = -\kappa\left(\frac{\partial T}{\partial y}\right)_{y=0} - \frac{4\sigma^*}{3k^*}\left(\frac{\partial T^4}{\partial y}\right)_{y=0},$$

$$m_w = -\rho D\left(\frac{\partial C}{\partial y}\right)_{y=0} \tag{16}$$

Using (16), quantity (15) can be written as

$$\begin{aligned} &C_{fx} = -2\,\mathrm{Re}_x^{-1/2} f''(0), \qquad Nu_x/\mathrm{Re}_x^{1/2} = -(1+R)\theta'(0), \\ &Sh_x/\mathrm{Re}_x^{1/2} = -\phi'(0) \end{aligned} \tag{17}$$

where $\mathrm{Re}_x = U_w x/\upsilon$ is the local Reynolds number based on the surface velocity.

We note that for $A = 0$, and in absence of heat source/sink and thermal radiation, the problem under consideration reduces to steady-state flow, where the closed-form solutions for the flow, thermal and concentration fields in terms of Kummer's functions are respectively given by [25]

$$f(\eta) = \varsigma - \frac{1}{\varsigma}e^{-\varsigma\eta} \tag{18}$$

$$\theta(\eta) = \frac{M\left(\Pr-1, \Pr+1, -\Pr\cdot e^{-\varsigma\eta}/\varsigma^2\right)}{M\left(\Pr+1, \Pr-1, -\Pr/\varsigma^2\right)} \tag{19}$$

$$\phi(\eta) = \frac{M\left(Sc-1, Sc+1, -Sc\cdot e^{-\varsigma\eta}/\varsigma^2\right)}{M\left(Sc+1, Sc-1, -Sc/\varsigma^2\right)} \tag{20}$$

where $f_w = \varsigma - \frac{1}{\varsigma}$ (with $\varsigma > 0$), and $0 < \varsigma < 1$ and $\varsigma > 1$ correspond to injection and suction, respectively. In Eqs. (19) and (20), $M(a,b,z)$ denotes the confluent hypergeometric function [28] as follows:

$$M(a,b,z) = 1 + \sum_{n=1}^{\infty}\frac{a_n z^n}{b_n n!} \tag{21}$$

where

$$\begin{aligned} &a_n = a(a+1)(a+2)................(a+n-1), \\ &b_n = b(b+1)(b+2)................(b+n-1). \end{aligned} \tag{22}$$

Using (14), we have from Eq. (18)

$$f(0) = f_w = \varsigma - \frac{1}{\varsigma}$$

Using (18) to (20), the skin friction coefficient $f''(0)$, the local Nusselt number $-\theta'(0)$ and the local Sherwood number $-\phi'(0)$ are given by

$$f''(0) = -\varsigma \tag{23}$$

$$\theta'(0) = -\varsigma\Pr + \frac{\Pr-1}{\Pr+1}\frac{\Pr}{\varsigma}\frac{M\left(\Pr, \Pr+2, -\Pr/\varsigma^2\right)}{M\left(\Pr-1, \Pr+1, -\Pr/\varsigma^2\right)} \tag{24}$$

$$\phi'(0) = -\varsigma Sc + \frac{Sc-1}{Sc+1}\frac{Sc}{\varsigma}\frac{M\left(Sc, Sc+2, -Sc/\varsigma^2\right)}{M\left(Sc-1, Sc+1, -Sc/\varsigma^2\right)} \tag{25}$$

3. Numerical Solution

Equations (11) to (13) subject to boundary conditions (14) are solved numerically using an implicit finite difference scheme, known as the Keller-box. This method found to be very suitable in dealing with nonlinear parabolic problems as discussed in the book by Cebeci and Bradshaw [29]. This solution procedure can be summarized by the following four steps :

1. Reduce equations (11) to (13) to a first-order system by introducing the new dependent variables.
2. Write the difference equations using central differences.
3. Linearize the resulting algebraic equations by Newton's method and write them in matrix-vector form.
4. Use the block-tridiagonal-elimination technique, solve the linear system obtained.

Here, the grid size in η of 0.01 is found to be satisfactory for a convergence criterion of 10^{-5} which gives accuracy to four decimal places. The satisfaction of the outer boundary condition is achieved by considering the boundary layer thickness $\eta_\infty = 6$. The correctness of our numerical method is checked with the results of Ishak et al. [24] and Pal [25] as shown in Table 1. It can be seen from this table that a very good agreement between the numerical results exist.

Table 1. Comparison of $-\theta'(0)$ for various values of $A,$ ς and Pr with previous published results when A* = B* = R = 0.

A	ς	Pr	Ishak et al. [24]	Pal [25]	Exact solution (Eq. (24))	Present
0	0.5	0.72	0.4570	0.457026833	0.457026833	0.4570
		1.0	5.0000	0.500000000	0.500000000	5.0000
		10.0	0.6452	0.645161290	0.645161289	0.6452
	1.0	0.01	0.0197	0.019706795	0.019706354	0.0197
		0.72	0.8086	0.808631352	0.808631350	0.8086
		1.0	1.0000	1.000000000	1.000000000	1.0000
		3.0	1.9237	1.923682561	1.923682594	1.9237
		10.0	3.7207	3.720673903	3.720673901	3.7207
		100.0	-	12.29408344	12.29408326	12.2940
	2.0	0.72	1.4944	1.494368414	1.494368413	1.4944
		1.0	2.0000	2.000000000	2.000000000	2.0000
		10.0	16.0842	16.08421882	16.08421885	16.0842
1.0	0.5	1.0	0.8095	0.809511470		0.8095
	1.0		1.3205	1.320522071		1.3205
	2.0		2.2224	2.222355356		2.2224

4. Result and Discussion

In this study, Figs. 1-3 present the velocity $f'(\eta)$, temperature $\theta(\eta)$ and concentration profiles $\phi(\eta)$ for different values of unsteadiness parameter A, respectively. These results show that the velocity, temperature and concentration profiles decrease with an increasing of unsteadiness parameter A. These show the important fact that the rate of cooling is much faster for higher values of unsteadiness parameter whereas it may take longer time for cooling during steady flows.

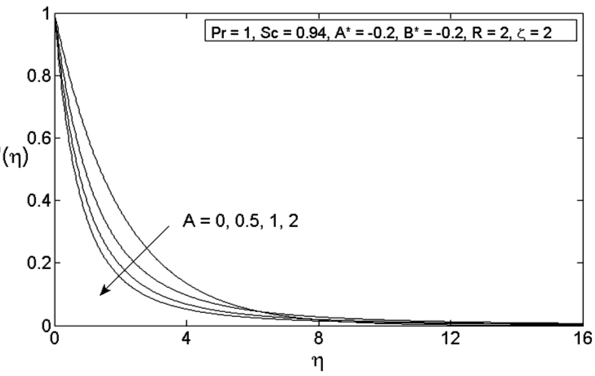

Fig. 1. Velocity profiles for different A.

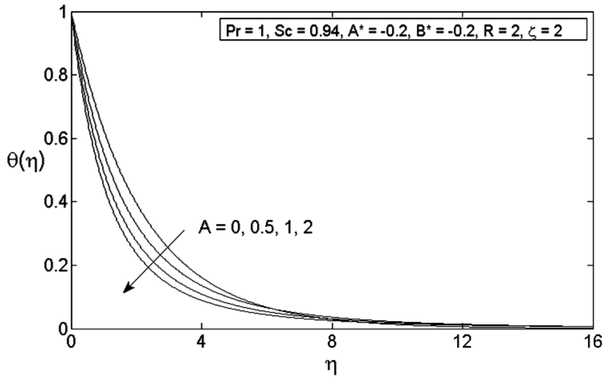

Fig. 2. Temperature profiles for different A.

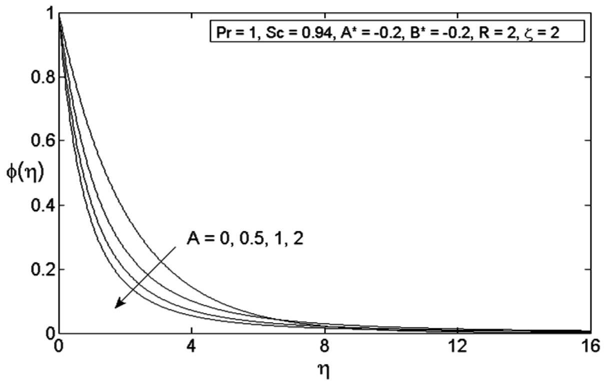

Fig. 3. Concentration profiles for different A.

The effect of suction/injection parameter ς on the velocity, temperature and concentration profiles, respectively are illustrated in Figs. 4-6. From these results, it is observed that the velocity, temperature and concentration profiles decrease with increasing values of suction/injection parameter. This is due to the fact that the suction have tendency to reduce the boundary layer thicknesses.

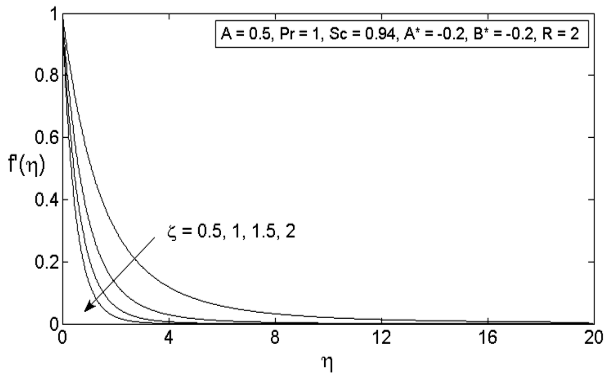

Fig. 4. Velocity profiles for different ς.

Fig. 7 illustrates the effect of heat source/ sink parameter A^* against unsteadiness parameter A on local Nusselt number. This figure shows that the local Nusselt number decreases with increasing heat generation $\left(A^* > 0\right)$ parameter, whereas reverse effect is observed for heat absorption $\left(A^* < 0\right)$ parameter. It is also noted that the heat source/sink parameter increases with increasing the unsteadiness parameter.

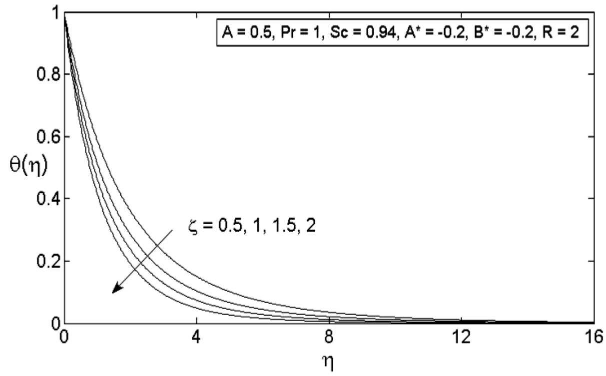

Fig. 5. Temperature profiles for different ς.

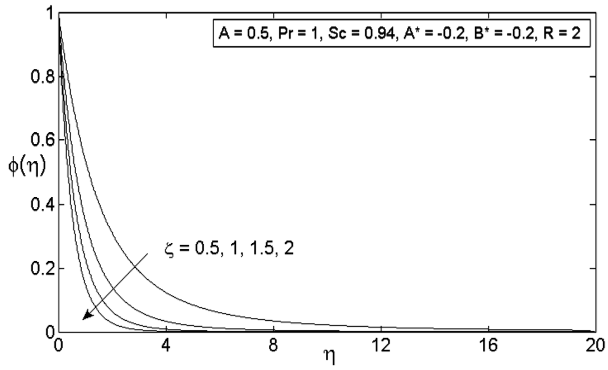

Fig. 6. Concentration profiles for different ς.

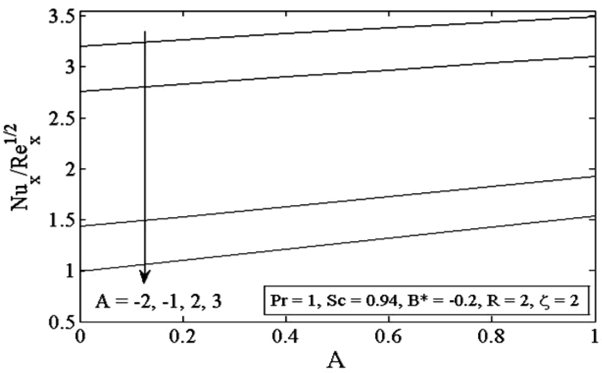

Fig. 7. Nusselt number for different A* versus A.

Fig. 8 depicted the variation of heat source/ sink parameter B^* against unsteadiness parameter A on local Nusselt number. From this figure, it is observed that local Nusselt number increases with increasing heat absorption

$(B^* < 0)$ parameter, whereas reverse effect is observed for heat generation $(B^* > 0)$ parameter. It is also noted that the heat source/sink parameter increases with increasing the unsteadiness parameter.

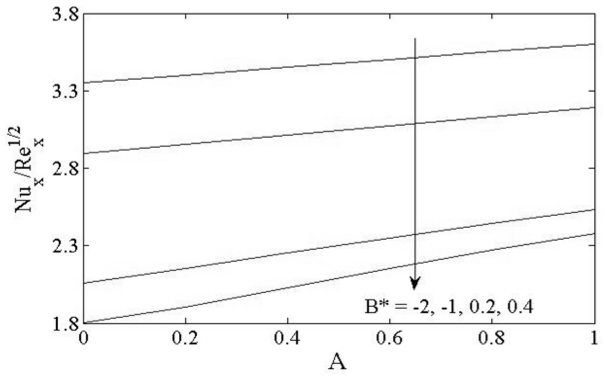

Fig. 8. Nusselt number for different B^* versus A.

Fig. 9 represents the local Nusselt number for different values of radiation parameter R against Prandtl number Pr. It is observed that the local Nusselt number increases with increasing Prandtl number. Further, it is noted that there is rapid increase in local Nusselt number with increase in the value of unsteadiness parameter.

The effect of Schmidt number on the local Sherwood number Sc against unsteadiness parameter A is illustrated in Fig. 10. From this figure, it is observed that the local Sherwood number increases with an increase in the value of Schmidt number. It is also noted that the local Sherwood number increases with increasing unsteadiness parameter.

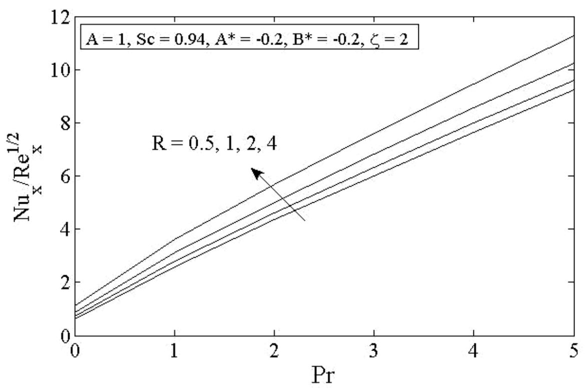

Fig. 9. Nusselt number for different R versus Pr.

Finally, the values of the Sherwood number are tabulated in Table 2 for various values of A and Sc. It is noted from this Table that local Sherwood number increases with increase in the value of A.

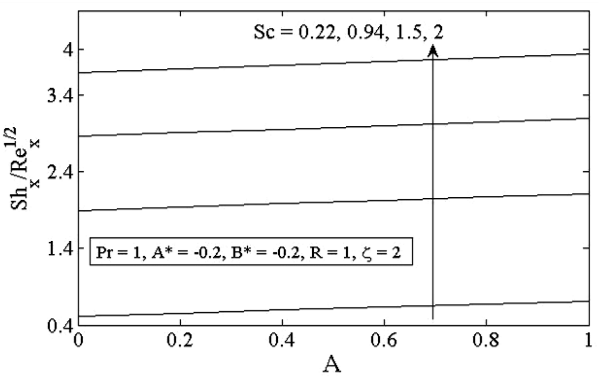

Fig. 10. Sherwood number for different Sc versus A.

Table 2. Computed of values of the local Sherwood number for various A and Sc when $\varsigma = 2, R = 1, \ A^* = 0.2, B^* = 0.2$.

A	Sc	Present results
0	0.22	0.5124
	0.94	1.8934
0.6	0.22	0.6372
	0.94	2.0266
1.0	0.22	0.7073
	0.94	2.1148

4. Conclusion

The present study provides the combined effects of heat and mass transfer over an unsteady stretching permeable surface with non-uniform source/sink and thermal radiation. The numerical results obtained and compared with previous published results and found in good agreements. In the light of present investigation, we found that the velocity, temperature and concentration decrease with increasing unsteadiness parameter. In addition, the local Nusselt number decreases with increasing heat source/sink parameter, while reverse trend is seen for radiation parameter. Further, the local Sherwood number increases with increase in the value of Schmidt number.

Acknowledgement

We are thankful to the editor and the referee for making constructive suggestions, which have improved the presentation of this work.

References

[1] L.J. Crane, J. Appl. Math Phys. **21** (1970) 645.

[2] P.S. Gupta and A.S. Gupta, Can. J. Chem. Eng. **55** (1977) 744.

[3] L.J. Grubka and K.M. Bobba, ASME J. Heat Transfer **107** (1985) 248.

[4] C.-K. Chen and M.-I. Char, J. Math. Anal. Appl. **135** (1988) 568.

[5] M.E. Ali, Heat Mass Transf. **29** (1994) 227.

[6] M.-I. Char, Heat Mass Transf. **29** (1994) 495.
[7] C.-H. Chen, Heat Mass Transf. **33** (1998) 471.
[8] A. Ishak, R. Nazar, and I. Pop, ASME J. Heat Transf. **129** (2007) 1087.
[9] A. Ishak, R. Nazar and I. Pop, Heat Mass Transf. **44** (2008) 921.
[10] C.Y. Wang, Nonlinear Anal. RWA. **10** (2009) 375.
[11] T. Fang, J. Zhang and Y. Zhong, Appl. Math. Comput. **218** (2012) 7241.
[12] S. Mukhopadhyay, Int. J. Heat Mass Transf. **52** (2009) 3261.
[13] D. Pal and M.S. Malashetty, Int. J. Appl. Mech. Eng.**13** (2008) 427.
[14] M.A. Hossain and H.S. Takhar, Int. J. Heat Mass Transf. **31** (1996) 243.
[15] H.S. Takhar, R.S.R. Gorla and V.M. Soundalgekar, Int. J. Numer. Meth. Heat Fluid Flow **6** (1996) 77.
[16] D. Pal, Meccanica **44** (2009) 145.
[17] Z. M. Yusof, S. K. Soid, A. S. Abd Aziz and S. A. Kechil, World Acad. Sci. Eng. Tech. **6** (2012) 1727.
[18] E.M. Abo-Eldahab and M.A. El-Aziz, Int. J. Theor. Sci. **43** (2004) 709.
[19] D. Pal and H. Mondal, Commun. Nonlinear Sci. Numer. Simul. **15** (2010) 1533.
[20] G. M. Pavithra and B. J. Gireesha, J. Mathematics **2013** (2013).
[21] T.Y. Na and I. Pop, Mech. Res. Comm. **23** (1996) 413.
[22] C.Y. Wang, G. Du, M. Miklavi and C.C. Chang, SIAM J. Appl. Math. **57** (1997) 1.
[23] E.M.A. Elbashbeshy and M.A.A. Bazid, Appl. Math. Comput., **138** (2003) 239.
[24] A. Ishak, R. Nazar and I. Pop, Nonlinear Anal: Real World Appl. **10** (2009) 2909.
[25] D. Pal, Comm. Nonlinear Sci. Numer. Simulat. **16** (2011) 1890.
[26] Y.I. Seini, J. Eng. Manufac. Tech. **1** (2013) 24.
[27] A. Raptis, Int. Comm. Heat Mass Transf. **25** (1998) 289.
[28] M. Abramowitz and I.A. Stegun, Handbook of Mathematical Functions, New York, Dover (1965).
[29] T. Cebeci and P. Bradshaw, Physical and Computational Aspects of Convective Heat Transfer (Springer, New York, 1988).